arXiv:hep-lat/0311030v2 12 Dec 2003

Nonperturbative renormalisation of composite operators with overlap quarks*

J. B. Zhang[a], D. B. Leinweber[a], K. F. Liu[b], A. G. Williams[a]

[a]CSSM Lattice Collaboration,
Special Research Center for the Subatomic Structure of Matter (CSSM) and Department of Physics, University of Adelaide 5005, Australia

[b]Department of Physics and Astronomy, University of Kentucky, Lexington, KY 40506

We compute non-perturbatively the renormalisation constants of composite operators on a $16^3 \times 32$ lattice with lattice spacing $a = 0.093$ fm for the overlap fermion action by using the regularisation independent (RI) scheme. The quenched gauge configurations are generated by tadpole improved plaquette plus rectangle action. We test the perturbative continuum relation $Z_A = Z_V$ and $Z_S = Z_P$ and find that they agree well above $\mu = 1.6$ GeV. We also perform a Renormalisation Group analysis at the next-to-next-to-leading order and convert the renormalisation constants to the $\overline{MS}$ scheme.

1. INTRODUCTION

Lattice QCD is a unique tool with which we can compute physical observables non-perturbatively from first principles. Renormalisation of lattice operators is an essential ingredient needed to deduce physical results from numerical simulations. In this paper we study the renormalisation properties of composite bilinear operators with the overlap quark action.

In principle, the renormalisation of a quark bilinear can be computed by lattice perturbation theory. However, lattice perturbation theory converges slowly and the higher-order corrections may not be small, thus introducing a large uncertainty in the calculation of the renormalised matrix elements in some continuum scheme. To overcome these difficulties, Martinelli *et al.* [1] have proposed a promising non-perturbative renormalisation procedure. The procedure allows a full non-perturbative computation of the matrix elements of composite operators in the Regularisation Independent (RI) scheme [1,2]. The matching between the RI scheme and $\overline{MS}$, which is intrinsically perturbative, is computed using only continuum perturbation theory and has been carried out to higher orders, which is well behaved. This method has been shown to be quite successful in reproducing results obtained by other methods, such as using chiral Ward Identities (WI) [3]. The method has also been successfully applied to determine renormalisation coefficients for various operators using the Wilson [4,5,6,7] and staggered actions [8], domain-wall fermions [9], as well as the quark mass renormalisation constant for overlap fermions [10]. The purpose of the current work is to study the application of this non-perturbative renormalisation procedure to the renormalisation of the quark field and the flavour non-singlet fermion bilinear operators in the case of overlap fermions.

We shall use Neuberger's overlap fermions [11] which have lattice chiral symmetry at finite cutoff. As a result, many chiral-symmetry relations are still valid [12,13] and the quark propagator [14] preserves the same structure as in the continuum. The use of the overlap action entails many theoretical advantages [15,16], such as no additive mass renormalisation, no $\mathcal{O}(a)$ error, and no mixing among operators of different chirality. The latter is very helpful for computing weak matrix elements.

2. NON-PERTURBATIVE RENORMALIZATION METHOD

In this section we review the nonperturbative renormalisation method of Ref. [1], which

*Presented by J. B. Zhang

we use to compute the renormalisation constants of quark bilinears in this paper. The method imposes renormalisation conditions non-perturbatively, directly on quark and gluon Green's functions, in a fixed gauge, for example the Landau gauge.

Let $S(x,0)$ denotes the quark propagator on a gauge-fixed configuration from a source 0 to all space-time points x. The momentum space propagator is defined as the discrete Fourier transform over the sink positions

$$S(p,0) = \sum_x \exp(-ip\cdot x)\, S(x,0)\ . \tag{1}$$

We use periodic boundary conditions in spatial directions and an anti-periodic boundary condition in time direction. The dimensionless lattice momenta are

$$p_i = \frac{2\pi}{N_s}(n_i - \frac{N_S}{2})\,,\quad p_t = \frac{2\pi}{N_t}(n_t - \frac{1}{2} - \frac{N_t}{2}) \tag{2}$$

for an $N_s^3 \times N_t$ lattice, where n_i (n_t) may in principle lie in the range $0 \to N_s(N_t)$. In practice, however, only a subset of this range is used. In this paper the momentum range was restricted to those momenta for which $n_i = 0,1,2$ and $n_t = 1,2,3,4$.

We also define the square of the absolute momentum,

$$(pa)^2 = a^2 \sum_{\mu=0}^{3} p_\mu\, p_\mu\,. \tag{3}$$

2.1. Three Point Function

Consider the two-fermion operators

$$O_\Gamma(x) = \bar\psi(x)\Gamma\psi\,, \tag{4}$$

where Γ is the Dirac gamma matrix

$$\Gamma \in \{1, \gamma_\mu, \gamma_5, \gamma_\mu\gamma_5, \sigma_{\mu\nu}\}\ , \tag{5}$$

and the corresponding notation will be {S, V, P, A, T} respectively. The three point function with the operator insertion at position 0 and the propagator from y to 0 and then from 0 to x is given by

$$\begin{aligned} G_O(x,0,y) &= \langle \psi(x) O_\Gamma(0) \bar\psi(y)\rangle \\ &= \langle S(x,0)\Gamma S(0,y)\rangle\,, \end{aligned} \tag{6}$$

where $S(0,y)$ is the quark propagator from y to 0. It is the inverse of the Dirac operator.

The Fourier transform of the three-point function is given by

$$\begin{aligned} G_O(pa,qa) &\equiv \int d^4x d^4y e^{-i(p\cdot x - q\cdot y)} G_O(x,0,y) \\ &= \langle S(p,0)\Gamma\left(\gamma_5 S^\dagger(q,0)\gamma_5\right)\rangle\,. \end{aligned} \tag{7}$$

From this, one can define the amputated three-point function

$$\Lambda_O(pa,qa) = S(pa)^{-1} G_O(pa,qa) S(qa)^{-1}\,, \tag{8}$$

where

$$S(pa) = \langle S(p,0)\rangle\,, \tag{9}$$

which is translational invariant and a 12×12 matrix.

Finally, we define a projected vertex function

$$\Gamma_O(pa) = \frac{1}{\mathrm{Tr}(\hat P_O^2)}\mathrm{Tr}\left(\Lambda_O(pa,pa)\hat P_O\right)\,, \tag{10}$$

where $\hat P_O = \Gamma$ is the corresponding projection operator.

2.2. RI/MOM Renormalisation Condition

The renormalised operator $O(\mu)$ at scale μ is related to the bare operator

$$O(\mu) = Z_O(\mu a, g(a)) O(a)\,, \tag{11}$$

and the renormalisation condition is imposed on the vertex function $\Gamma_O(pa)$ at a scale $p^2 = \mu^2$,

$$\Gamma_{O,\mathrm{ren}}(pa)|_{p^2=\mu^2} = \frac{Z_O}{Z_\psi}\Gamma_O(pa)|_{p^2=\mu^2} = 1\,, \tag{12}$$

to make it agree with the tree-level value of unity. Here Z_ψ is the field or wavefunction renormalisation

$$\psi_{\mathrm{ren}} = Z_\psi^{1/2}\psi\,. \tag{13}$$

In order to obtain the renormalisation constant Z_O for the operator O, one needs to know Z_ψ first. It has been suggested that Z_ψ be obtained from the renormalisation of vector or axial-vector currents. For example, if one uses the conserved vector current, then one expects $Z_{V^C} = 1$. Therefore, from the renormalisation condition Eq. (12), one obtains,

$$Z_\psi = \frac{1}{48}\mathrm{Tr}\left(\Lambda_{V_\mu^C}(pa)\gamma_\mu\right)|_{p^2=\mu^2}\,. \tag{14}$$

However, in this work, we will obtain Z_ψ directly from the quark propagator. It can be defined from the Ward Identity (WI) as [1]

$$Z_\psi = -i\frac{1}{12}\mathrm{Tr}\left[\frac{\partial S(pa)^{-1}}{\partial\!\!\!/ p}\right]\,|_{p^2=\mu^2}\ . \qquad (15)$$

To avoid derivatives with respect to a discrete variable, we have used

$$Z'_\psi = -i\frac{1}{12}\frac{\mathrm{Tr}\sum_{\mu=1,4}\gamma_\mu(p_\mu a)S(pa)^{-1}}{4\sum_{\mu=1,4}(p_\mu a)^2}\Bigg|_{p^2=\mu^2}\ , (16)$$

which, in the Landau Gauge, differs from Z_ψ by a finite term of order α_s^2 [17], and the difference is less than 1% at the typical scale $\mu \sim 2$ GeV. It has been pointed out in Ref. [9] that the systematic error due to the definition of lattice momentum p is much larger than 1%. We will not distinguish Z'_ψ and Z_ψ later on.

3. NUMERICAL RESULTS

We work on a $16^3 \times 32$ lattice with lattice spacing, a=0.093 fm. The gauge configurations are created using a tadpole improved plaquette plus rectangle (Lüscher-Weisz [18]) gauge action through the pseudo-heat-bath algorithm. A total of 50 configurations are considered. The lattice parameters are summarised in Table 1. The lattice spacing is determined from the static quark potential with a string tension $\sqrt{\sigma} = 440$ MeV [19].

Table 1
Lattice parameters.

Action	Volume	N_{Samp}	β	a (fm)
Improved	$16^3 \times 32$	500	4.80	0.093

The gauge field configurations are gauge fixed to the Landau gauge using a Conjugate Gradient Fourier Acceleration [20] algorithm with an accuracy of $\theta \equiv \sum |\partial_\mu A_\mu(x)|^2 < 10^{-12}$. We use an improved gauge-fixing scheme [21] to minimise gauge-fixing discretisation errors.

The massive overlap Dirac operator [11] is defined so that at tree-level there is no mass or wavefunction renormalisation [22],

$$D(m_0) = \rho + \frac{m_0}{2} + (\rho - \frac{m_0}{2})\gamma_5\epsilon(H)\,. \qquad (17)$$

Here $\epsilon(H) = H/\sqrt{H^2}$ is the matrix sign function and H is taken to be the hermitian Wilson-Dirac operator, *i.e.*, $H = \gamma_5 D_{\mathrm{W}}$. Here D_{W} is the usual Wilson fermion operator, but with a negative mass parameter $-\rho = 1/2\kappa - 4$ in which $\kappa_c < \kappa < 0.25$.

Our numerical calculation begins with an evaluation of the inverse of $D(m_0)$ for each gauge configuration in the ensemble. We use a 14th order Zolotarev approximation [23] to the sign matrix function $\epsilon(H_w)$, and in the selected window of $x \in [0.031, 2.5]$ of $\epsilon(x)$, the approximation is better than 3.3×10^{-10} [24]. In the calculations, $\kappa = 0.19163$ is used, which gives $\rho a = 1.391$. We calculate 15 quark masses by using a shifted version of a Conjugate Gradient solver. The bare quark masses $m_0 a$ are chosen to be 0.0250, 0.0278, 0.0334, 0.0389, 0.0445, 0.0501, 0.0584, 0.0668, 0.0834, 0.1001, 0.1252, 0.1669, 0.2086, 0.2503, 0.2921. The m_0 values in physical units are 53, 59, 71, 83, 94, 106, 124, 142, 177, 212, 266, 354, 442, 531, and 620 MeV respectively.

3.1. Axial and vector currents

Let us consider first the vector and axial vector currents. Since each obeys a chiral WI [25] their renormalisation constants are finite. In Fig. 1, we show Γ_A and Γ_V, calculated in the RI scheme for different bare quark masses as a function of the lattice momentum $(pa)^2$. We find they are weakly dependent on the mass, and almost scale independent for $(pa)^2 \geq 0.5$.

For the overlap fermion, which satisfies the Ginsparg-Wilson [26] relation and preserves chiral symmetry on finite lattice. In Ref. [27] it has been proved that the renormalisation constants for naive vector and axial vector currents satisfy

$$Z_A = Z_V\,. \qquad (18)$$

In Fig. 2 we show the quantities $\Gamma_A - \Gamma_V$ and and $\frac{1}{2}(\Gamma_A + \Gamma_V)$, after extrapolating to the chiral limit. We can see from upper part of the figure that there is no signal of effects from chiral symmetry breaking, since $\Gamma_A - \Gamma_V$ is tending to zero at moderate and high momenta. The effects of spontaneous chiral symmetry breaking are visible at low momenta and they are damped at higher momenta. At the momenta of interest, there also

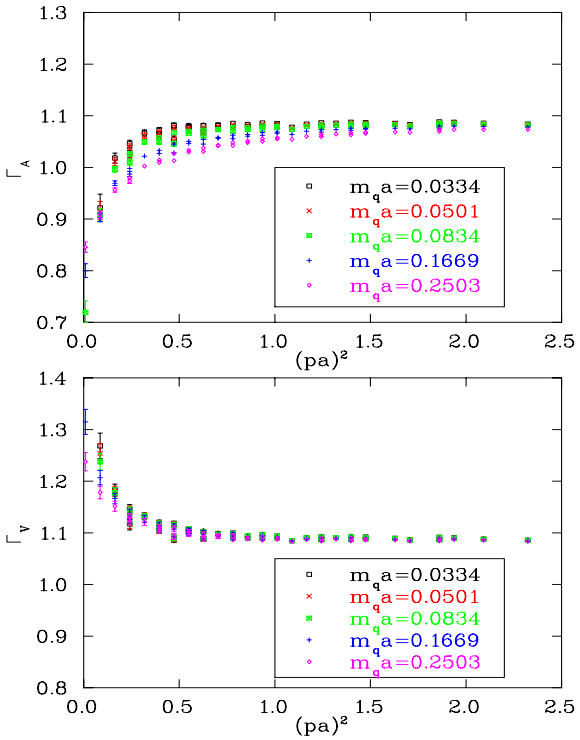

Figure 1. The projected vertex function Γ defined in Eq. (10) for vector and axial vector currents with different bare quark masses. By the renormalisation condition (Eq.(12)), they are the ratio of renormalisation constant Z_ψ/Z_A and Z_ψ/Z_V respectively.

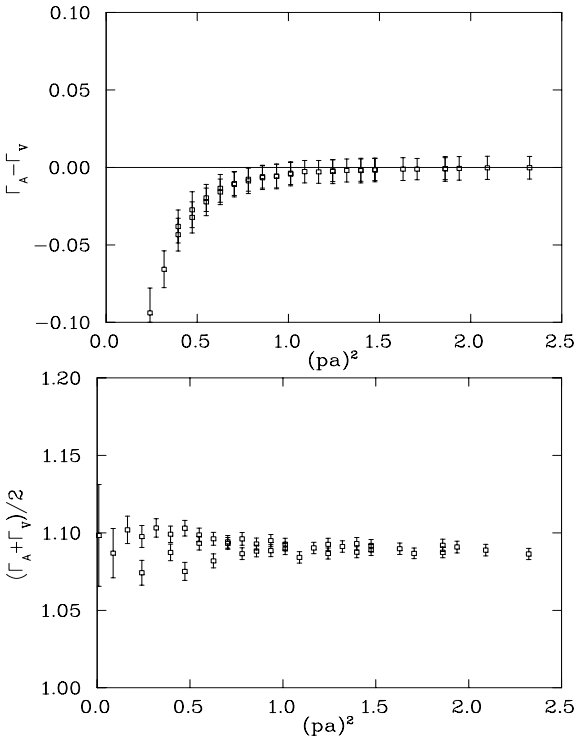

Figure 2. Checking $Z_A = Z_V$, the upper plot is $(\Gamma_A - \Gamma_V)$ versus $(pa)^2$, where we linear extrapolate to the chiral limit ($m_0 = 0$). The lower plot is $\frac{1}{2}(\Gamma_A + \Gamma_V)$ versus $(pa)^2$. The relation $Z_A = Z_V$ is valid at moderate to large $(pa)^2$.

seems to be no significant splitting due to non-perturbative effects with the difference between Γ_A and Γ_V being less than 1% at $(ap)^2 = 0.7$ and smaller for momenta above this. In the lower part of Fig. 2, we plot $\frac{1}{2}(\Gamma_A + \Gamma_V)$ against $(ap)^2$, and it can be used for the extraction of both Z_A/Z_ψ and Z_V/Z_ψ to increase the statistical accuracy.

3.2. Pseudoscalar and scalar densities

The pseudoscalar and scalar densities differ from the axial and vector currents in that their renormalisation is not scale independent. For overlap fermions with chiral symmetry the RI scheme preserves the well known $\overline{MS}$ relations

$$Z_S = Z_P \quad \text{and} \quad Z_m = \frac{1}{Z_S}\,, \tag{19}$$

and the quantities Z_S/Z_P, $Z_S Z_m$ and $Z_m Z_P$ are expected to be scale independent.

Fig. 3 and Fig. 4 show Γ_S and Γ_P versus $(pa)^2$ with different masses. Unlike in the case of the vector and axial vector currents, they are strongly dependent on the quark mass m_0 for light quarks. When we want to extract the chiral limit value, we cannot use a simple linear or quadratic fit. In Fig. 3 and Fig. 4, we can clearly see the pole effect in the small $(pa)^2$ region.

As discussed in detail in Ref. [9], due to the contribution from the zero-modes, we may fit the Γ_S to the form

$$\Gamma_S = \frac{c_{1,S}}{(am_0)^2} + c_{2,S} + c_{3,S}(am_0)^2 \tag{20}$$

at a fixed momentum with Z_ψ/Z_S being given by $c_{2,S}$. The fitted value of $c_{2,S}$ is plotted in Fig. 5 as Z_ψ/Z_S. We find that the coefficient of the pole term, $c_{1,S}$ is very small, between 10^{-3} to 10^{-4}, this means that the pole term only provides a

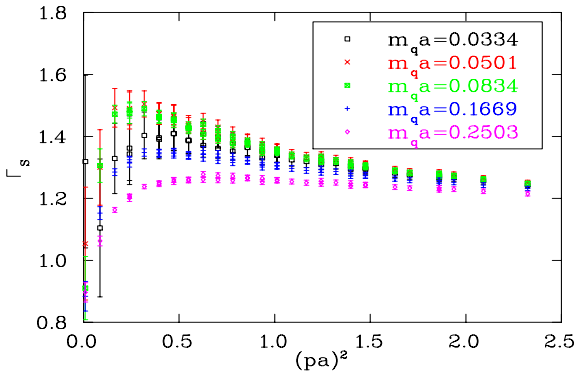

Figure 3. Γ_S versus $(pa)^2$ with different masses. Here one can see the strong mass dependence and non-monotonic behaviour.

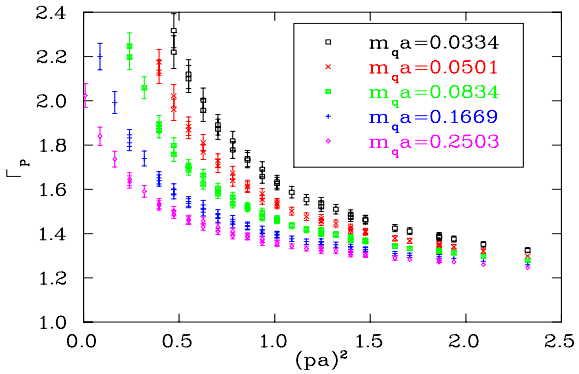

Figure 4. Γ_P versus $(pa)^2$ with different masses. Here also we have strong mass dependence and pole behaviour.

large contribution at very small m_0, i.e., near the chiral limit.

For Γ_P, we fit to the form

$$\Gamma_{P,\mathrm{latt}} = \frac{c_{1,P}}{(am_0)^2} + \frac{c_{2,P}}{(am_0)} + c_{3,P} + c_{4,P}(am_0)^2 \,, \quad (21)$$

with $c_{3,P}$ being equal to Z_ψ/Z_P. The quadratic mass pole is due to zero-mode effects in $\langle \overline{q}q \rangle$. The fitted value of $c_{3,P}$ is plotted in Fig. 5 as Z_ψ/Z_P.

As the evidence for the above fitting form, we consider the resulting values for Z_ψ/Z_S and Z_ψ/Z_P. Fig. 5 shows a comparison between the extracted values of these two quantities. As chiral symmetry would predict for Z_ψ/Z_S and Z_ψ/Z_P, the two quantities coincide at moderate and large momenta.This provides an excellent test of both the fitting method to extract the poles and the

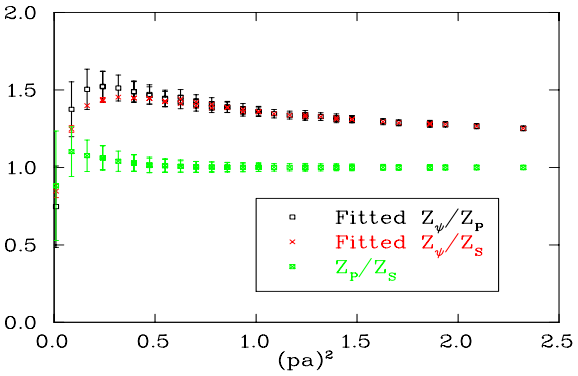

Figure 5. Checking of $Z_P = Z_S$ after mass pole subtraction.

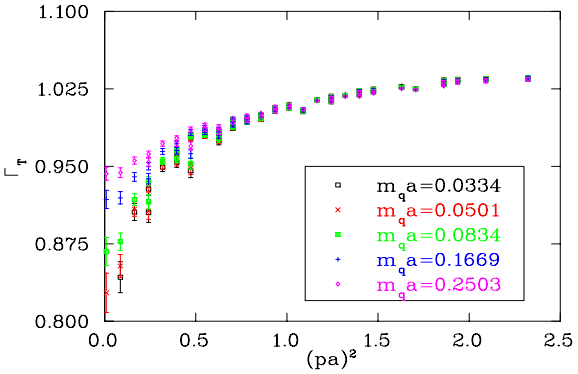

Figure 6. Γ_T versus $(pa)^2$ with different masses. It shows no significant mass dependence for moderate to large $(pa)^2$.

chiral properties of overlap fermions.

3.3. The Tensor current

In Fig. 6 we show Γ_T versus $(pa)^2$ with different masses. We can see that at moderate and large $(pa)^2$, Γ_T is not sensitive to the quark masses. The chiral limit value is obtained by a linear fit in quark mass as for the cases of vector and axial vector currents, and the results will be presented in the next subsection.

3.4. Running of the renormalisation constants

The renormalised operators are defined as

$$Z_O O_{\mathrm{bare}} = O_{\mathrm{ren}} \,. \quad (22)$$

Requiring the bare operator to be independent of the renormalisation scale μ^2 gives the RG equa-

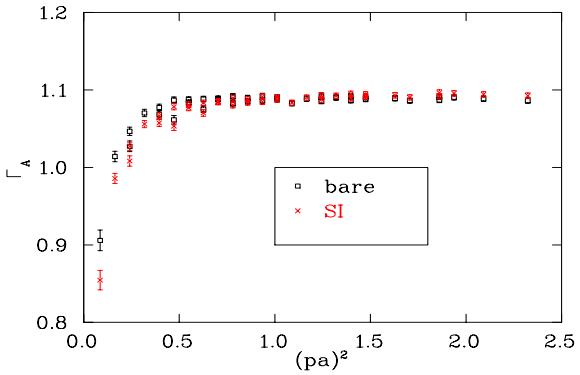

Figure 7. Γ_A versus $(pa)^2$ in the chiral limit before (labelled as "bare") and after (labelled as "SI") three loop perturbative running, such that they coincide at $(pa)^2 = 1$. The latter is almost $(pa)^2$ independent after $(pa)^2 > 0.6$. The slope versus $(pa)^2$ is about 0.01 and is interpreted as an $O(a^2)$ effect.

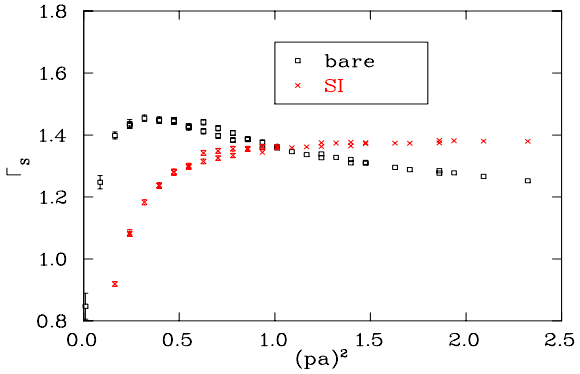

Figure 8. The same as Fig. (7). Here is Γ_S versus $(pa)^2$. The slope of SI versus $(pa)^2$ is about 0.02.

tion,

$$\mu^2 \frac{d}{d\mu^2} O_{\rm ren} = \frac{1}{Z_O} \mu^2 \frac{dZ_O}{d\mu^2} O_{\rm ren} = -\frac{\gamma_O}{2} O_{\rm ren} \,. \quad (23)$$

The solution of $Z_O(\mu^2)$ can be written in the following form

$$Z_O\left(\mu^2\right) = \frac{C_O\left(\mu^2\right)}{C_O\left(\mu'^2\right)} Z_O\left(\mu'^2\right) \,. \quad (24)$$

The coefficient $C_O\left(\mu^2\right)$ can be found in Appendix B of Ref. [9] and references within.

In this work, the value of α_s was calculated at three loops using a lattice value of $\Lambda_{\rm QCD}$ taken from Ref. [28] as $\Lambda_{\rm QCD} = 238 \pm 19 {\rm MeV}$.

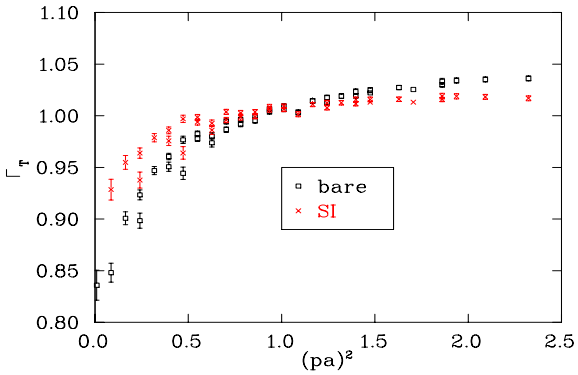

Figure 9. Γ_T versus $(pa)^2$ in the chiral limit before and after two loop perturbative running. The latter is almost $(pa)^2$ independent after $(pa)^2 > 0.6$, the slope versus $(pa)^2$ is about 0.01.

Both Z_A and Z_V should be scale independent, but this is not the case for Z_ψ. Fig. 7 shows both Γ_A and the scale invariant (SI) quantity (the data after removing the renormalisation group running) calculated as described above:

$$\Gamma_A^{SI}\left((ap)^2\right) = \Gamma_A\left((ap)^2\right) / C_\psi\left((ap)^2\right) \,. \quad (25)$$

The quantity C_ψ is normalised so that $C_\psi(1) = 1$. As can be seen, in this case the renormalisation group running is coming from Z_ψ alone. It is small, but it actually improves the scale independence of the data. The remain scale dependence of this data is very small and a plausible explanation for this is a small $(ap)^2$ error. Indeed, when a linear fit of the SI data versus $(ap)^2$ is performed, for $0.8 < (ap)^2 < 2.0$, the gradient is ≈ 0.01.

In the case of Z_ψ/Z_S, the two renormalisation constants are both running with $(ap)^2$. Fig. 8 shows both Γ_S and the scale invariant (SI) quantity after three loop running. The modification to the raw data, which is taken after the mass-pole has been subtracted gives a satisfactory result. The linear fit of the SI data versus $(ap)^2$ in the range of $0.8 < (ap)^2 < 2.3$, gives a gradient of about 0.02.

The SI result of Γ_T which comes from the two loop running of Z_T [29] and three loop running of Z_ψ is plotted in Fig. 9, The "bare" data is taken by a simple linear extrapolation to the chiral limit. The linear fit to the SI data gives gradient about 0.01.

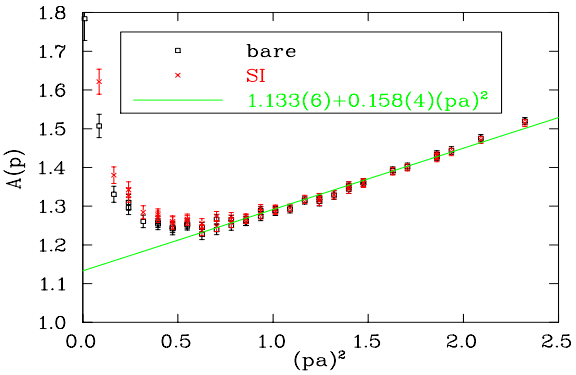

Figure 10. $A(p)$ in the chiral limit and its scale invariant counterpart versus $(pa)^2$ as $a + b\ (pa)^2$. The fitting range is [0.70, 2.32], which gives Z_ψ about 1.133 ± 0.006.

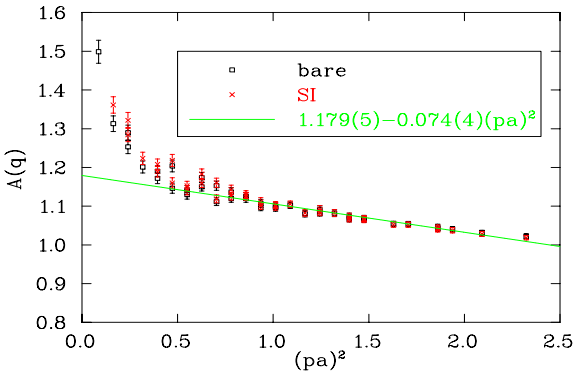

Figure 11. Z_ψ calculated from Eq. (15) by using the kinematic lattice momentum q_μ instead of the discrete lattice momentum p_μ.

With the interpretation that the remaining scale dependence is due to $\mathcal{O}(ap)^2$ effects, the correct way to extract the renormalisation coefficients is to first construct the SI quantity as described above, and then fit any remaining scale dependence [4] to the form

$$y = c_1 + c_2(ap)^2\,, \tag{26}$$

for a range of momenta that is chosen to be "above" the region for which condensate effects are important. We choose the range $0.8 < (ap)^2 < 2.3$. We then apply the renormalisation group running formula (an inverse operation of Eq. (25)) to c_1 in Eq. (26) to get the ratio of the renormalisation constant which is now free of $(ap)^2$ error in RI scheme.

3.5. Extracting Z_ψ from the propagator

Here we will use Eq. (16) to extract the wave function renormalisation constant Z_ψ. We will use two different definitions of lattice momenta, *i.e.* , the discrete lattice momentum defined in Eq. (2) and the kinematic lattice momentum q_μ which was introduced in Eq. (A9) of Ref. [30].

3.5.1. Discrete lattice momentum p_μ

We here use the discrete lattice momentum p_μ in Eq. (16) to calculate Z'_ψ. By using Eq. (16), we can get the corresponding quantity of Z'_ψ (here we use the symbol $A(p)$ for Z'_ψ). The resulting $A(p)$ is strongly dependent on the scale. We use three loop perturbative running in RI scheme and finally extract the value of Z_ψ from $A(p)$ by fitting $A(p)$ to Eq. (26) for a range of momenta for which the condensate effects are unimportant. Here we chose the range $(ap)^2 \subset (0.70, 2.32)$, which corresponds to $p \in (1.78, 3.23)$ GeV. c_1 can be identified as the SI value of Z_ψ. In Fig. 10 we show a linear fit for $A(p)$ versus $(pa)^2$ as in Eq. (26).

3.5.2. Kinematic lattice momentum q_μ

Another way to calculate Z_ψ is to use the kinematic lattice momentum q_μ defined in Eq. (A9) of Ref. [30]. The calculations are similar to those using p_μ. The result is plotted in Fig. 11. The fitted value of Z_ψ is 1.179(5), with the difference to the value calculated by p_μ being less than 4%. In both calculations, we attribute the remaining $(pa)^2$ dependence to the possible $\mathcal{O}((pa)^2)$ error and use the linear fit Eq.(26) to remove it. When using the kinematic lattice momentum q_μ to calculate Z_ψ, the $\mathcal{O}((pa)^2)$ errors are much smaller than in the case of using the discrete lattice momentum p_μ.

3.6. Matching to $\overline{MS}$ scheme

In order to confront experiment, one frequently prefers to quote the final results in the $\overline{MS}$ scheme at a certain scale. For light hadrons, the popular scale is 2 GeV.

The perturbative expansion of the ratio $Z^{\overline{MS}}/Z^{RI}$ to two-loop order is given by [4]

$$R = \frac{Z^{\overline{MS}}}{Z^{RI}} = 1 + \frac{\alpha_s}{4\pi}(Z^{RI})_0^{(1)} + (\frac{\alpha_s}{4\pi})^2(Z^{RI})_0^{(2)} + \ldots . \tag{27}$$

The numerical values of the matching coefficients, $Z_0^{(1)}$ and $Z_0^{(2)}$ in Eq. (27) for Z_ψ and Z_S can be found in Appendix C of Ref. [9], we have not found the numerical value for Z_T in the literature. The final results for the renormalisation constants are listed in Table 2.

Table 2
Final Z-factor results

$Z-$factor	RI (2 GeV)	$\overline{MS}$ at 2 GeV
Z_A/Z_ψ	0.924±0.004	0.928±0.004
Z_S/Z_ψ	0.739±0.003	0.842±0.004
Z_T/Z_ψ	1.009±0.002	1.012±0.002
$Z_\psi(from\ \ p)$	1.134±0.006	1.130±0.006
$Z_\psi(from\ \ q)$	1.180±0.005	1.175±0.005

4. SUMMARY

In this work we performed the non-perturbative renormalisation of composite operators with overlap fermions. The main results are: in $\overline{MS}$ scheme at $\mu = 2$ GeV, $Z_\psi = 1.153(5)(22)$, $Z_S = 0.970(4)(20)$, $Z_A = 1.070(5)(21)$, and $Z_T = 1.167(3)(23)$, where the first error is statistical and the second error comes from using the two different lattice momenta to get Z_ψ.

Support for this research from the Australian Research Council is gratefully acknowledged.

REFERENCES

1. G. Martinelli, C. Pittori, C.T. Sachrajda, M. Testa and A. Vladikas, Nucl. Phys. B 445, 81 (1995).
2. M. Ciuchini, E. Franco, G. Martinelli, L. Reina, L. Silvestrini, Z. Phys. C 68 , 239 (1995).
3. G. Martinelli, S. Petrarca, C.T. Sachrajda and A. Vladikas, Phys. Lett. B 311 , 241 (1993), E: B317, 660 (1993).
4. V. Gimenez, L. Giusti, F. Rapuano, M. Talevi, Nucl. Phys. B531, 429 (1998).
5. A. Donini, V. Gimenez, G. Martinelli, M. Talevi and A. Vladikas, Eur. Phys. J. C 10, 121 (1999).
6. L. Giusti *et al.*, Nucl. Phys. (Proc. Suppl.) B 73, 210 (1999).
7. D. Becirevic *et al.*, Phys. Lett. B 444, 401 (1998).
8. JLQCD Collaboration, S. Aoki *et al.*, Nucl. Phys. (Proc.Suppl.) B 73, 279 (1999).
9. T. Blum *et al.*, Phys. Rev. D **66**, 014504 (2002).
10. L. Giusti, C. Hoelbling, C. Rebbi, Phys. Rev. D, **64**, 114508 (2001). Erratum-ibid. D, **65**, 079903,(2002).
11. H. Neuberger, Phys. Lett. B417, 141 (1998), Phys. Lett. B427 353 (1998).
12. R. Narayanan, H. Neuberger, Phys. Lett. B302, 62 (1993), Nucl. Phys. B 443, 305 (1995).
13. M. Lüscher, Phys. Lett. B428, 342 (1998).
14. K.F. Liu, hep-lat/0206002.
15. H. Neuberger, Nucl. Phys. (Proc.Suppl.) B 83, 67 (2000).
16. S. J. Dong, F. X. Lee, K. F. Liu, and J. B. Zhang, Phys. Rev. Lett. 85, 5051 (2000).
17. E. Franco and V. Lubicz, Nucl. Phys. B531, 641 (1998)
18. M. Lüscher and P. Weisz, *Commun. Math. Phys.* **97**, 59 (1985).
19. F. D. R. Bonnet *et al.*, hep-lat/9912044.
20. A. Cucchieri and T. Mendes, Phys. Rev. D **57**, 3822 (1998).
21. F. D. R. Bonnet *et al.*, Austral J. Phys. **52**, 939 (1999).
22. S. J. Dong, T. Draper, I. Horváth, F. X. Lee, K. F. Liu, and J. B. Zhang, Phys. Rev. D **65**, 054507 (2002).
23. J. van den Eshof *et al.*, Comput. Phys. Commun. **146**, 203 (2002); Nucl. Phys. (Proc. Suppl.) **106**, 1070(2002).
24. S. J. Dong *et al.*, hep-lat/0304005
25. M. Bochicchio, L. Maiani, G. Martinelli, G.C. Rossi and M. Testa, Nucl. Phys. B 262, 331 (1985).
26. P. H. Ginsparg, K. G. Wilson, Phys. Rev. D, **25**, 2649 (1982).
27. C. Alexandrou, E. Follana, H. Panagopoulos, E. Vicari, Nucl. Phys. B 580, 394 (2000).
28. S. Capitani, M.Luscher, R. Sommer and H. Wittig, Nucl. Phys. B 544, 669 (1999),
29. J. A. Gracey, Nucl. Phys. B 667, 242 (2003).
30. F. D. R. Bonnet *et al.*, Phys. Rev. D **65**, 114503 (2002).